

Pseudomode expansion of many-body correlation functions

Alexander Teretenkov,^{1,2} Filipp Uskov,¹ and Oleg Lychkovskiy^{1,2}

¹*Skolkovo Institute of Science and Technology*

Bolshoy Boulevard 30, bld. 1, Moscow 121205, Russia

²*Department of Mathematical Methods for Quantum Technologies,*

Steklov Mathematical Institute of Russian Academy of Sciences

8 Gubkina St., Moscow 119991, Russia

(Dated: January 16, 2025)

We present an expansion of a many-body correlation function in a sum of pseudomodes – exponents with complex frequencies that encompass both decay and oscillations. The pseudomode expansion emerges in the framework of the Heisenberg version of the recursion method. This method essentially solves Heisenberg equations in a Lanczos tridiagonal basis constructed in the Krylov space of a given observable. To obtain pseudomodes, we first add artificial dissipation satisfying the dissipative generalization of the universal operator growth hypothesis, and then take the limit of the vanishing dissipation strength. Fast convergence of the pseudomode expansion is facilitated by the localization in the Krylov space, which is generic in the presence of dissipation and can survive the limit of the vanishing dissipation strength. As an illustration, we present pseudomode expansions of infinite-temperature autocorrelation functions in the quantum Ising and XX spin-1/2 models on the square lattice. It turns out that it is enough to take a few first pseudomodes to obtain a good approximation to the correlation function.

Introduction. Expanding a function into a functional series is a basic technique with countless applications in mathematics and theoretical physics. Typically, the convergence of the expansion is better (in terms of the domain and the rate) when the terms of the series share some general features of the function being expanded. For example, Fourier series are better suited for periodic functions, Taylor series – for polynomially growing functions *etc.* Choosing a suitable series can be decisive when an unknown function is found step by step by computing consecutive terms of the series.

Here we report an expansion technique for many-body time-dependent correlation functions. Generically correlation functions decay exponentially at large times, often with oscillations on top of the exponential decay [1–7]. It was therefore proposed to expand correlation functions in decaying modes $\text{Re } e^{\lambda_l t}$, where λ_l , $l = 0, 1, \dots$ are complex numbers with negative real parts [1–9].

Analogous expansions recurrently appeared in the studies of open systems interacting with large reservoirs [10–18]. Modes with complex frequencies were referred to as *pseudomodes* in some of these studies. We adopt this term, even though there are no explicit reservoirs in our setting.

Within a parallel line of research, it was argued [2, 6, 8] that complex modes emerge without any explicit reservoir as quantum analogs of classical Ruelle-Pollicott resonances [19, 20]. Recently, this research direction has been reinvigorated [9].

We present a concrete scheme to construct the pseudomode expansion based on (the Heisenberg version of) the recursion method [1, 21–23]. This method amounts to constructing a Lanczos basis in the Krylov space of operators and solving coupled Heisenberg equations in this basis. In the many-body case one additionally

has to extrapolate the sequence of Lanczos coefficients according to the universal operator growth hypothesis (UOGH) [24]. Recent years have witnessed a considerable progress in applying the recursion method to compute correlation functions in one [24–32] and two [32, 33] spatial dimensions.

To obtain the pseudomode expansion within the recursion method, we first add an artificial dissipation to the evolution superoperator, then diagonalize it and finally take the limit of vanishing dissipation strength. In fact, the usage of an auxiliary infinitesimal dissipation is ubiquitous in theoretical physics – in particular, it recurrently appears in various perturbative expansions and diagrammatic techniques [34, 35]. Variations of this trick have been used to track nonperturbative Heisenberg evolution [2, 8, 9, 36–41].

An important distinctive feature of our approach is the way we add the auxiliary dissipation. We do so directly in the Lanczos basis, and ensure that the dissipative term obeys the dissipative version of the UOGH [42–44]. Such a dissipative term leads to the localization in the Krylov space [43] (see also [44], [18]). In turn, the localization ensures the emergence of discrete pseudomodes and the fast convergence of the pseudomode expansion.

The rest of the paper is organized as follows. First we introduce the general formalism of the recursion method. After that we present the technique to compute pseudomode eigenvalues and amplitudes within the recursion method. Then we illustrate all major features of the technique, including localization and fast convergence, in a toy exactly solvable model of evolution superoperator. Finally, we explain how to practically construct the truncated pseudomode expansion starting from a many-body Hamiltonian, and illustrate the method by applying it to the quantum Ising and XX spin-1/2 models on the

square lattice.

Recursion method. Consider some observable given by a self-adjoint Schrödinger operator A . The same observable in the Heisenberg representation reads $A_t = e^{itH} A e^{-itH}$, where H is the Hamiltonian of the system. The Heisenberg operator A_t evolves within the *Krylov space* spanned by Schrödinger operators $A, \mathcal{L}A, \mathcal{L}^2A, \dots$, where $\mathcal{L} \equiv [H, \bullet]$ is the evolution *superoperator*. Knowledge of A_t allows one to compute time-dependent correlation functions related to this observable. Throughout the paper we focus on the simplest case of infinite-temperature autocorrelation function

$$C(t) \equiv \text{tr}(A A_t) / \text{tr} A^2. \quad (1)$$

It has the properties $C(0) = 1$ and $C(-t) = C(t)$.

We introduce a scalar product in the space of operators according to $(A|B) \equiv \text{tr}(A^\dagger B)/d$, where d is the Hilbert space dimension (which is assumed to be finite). The scalar product entails the norm $\|A\| = \sqrt{(A|A)}$. In this notation, the autocorrelation function can be written as $C(t) = (A|A_t)/\|A\|^2$. The superoperator \mathcal{L} is self-adjoint with respect to this scalar product.

The Heisenberg equation of motion reads $\partial_t A_t = i\mathcal{L}A_t$. In the recursion method [1, 21–23], this equation is addressed in the orthonormal Lanczos basis $\{O^0, O^1, O^2, \dots\}$ constructed as follows: $O^0 = A/\|A\|$, $A^1 = \mathcal{L}O^0$, $b_1 = \|A^1\|$, $O^1 = b_1^{-1}A^1$ and $A^n = \mathcal{L}O^{n-1} - b_{n-1}O^{n-2}$, $b_n = \|A^n\|$, $O^n = b_n^{-1}A^n$ for $n \geq 2$. The coefficients b_n are known as *Lanczos coefficients*. In this basis the evolution superoperator has a tridiagonal form,

$$\mathcal{L} = \begin{pmatrix} a_0 & b_1 & 0 & 0 & \dots \\ b_1 & a_1 & b_2 & 0 & \dots \\ 0 & b_2 & a_2 & b_3 & \dots \\ 0 & 0 & b_3 & a_3 & \dots \\ \vdots & \vdots & \vdots & \vdots & \ddots \end{pmatrix}, \quad (2)$$

where, for the moment, $a_n = 0$. The coupled Heisenberg equation can be conveniently written in matrix form as

$$\partial_t O_t = i\mathcal{L}O_t, \quad O_0 = O, \quad (3)$$

where $O_t = \|O_t^n\|_{n=0,1,2,\dots}$ is a column vector constructed of Heisenberg operators O_t^n and $O = \|O^n\|_{n=0,1,2,\dots}$ is a column vector constructed of Schrödinger operators O^n .

In practice, one can explicitly compute only a finite number n_{\max} of Lanczos coefficients. The rest of the coefficients should be extrapolated. The extrapolation is facilitated by the universal operator growth hypothesis [24] (see also a precursor work in [45–47]) which states that in a generic quantum many-body system b_n scales linearly with n at large n (with a logarithmic correction for one-dimensional systems). This asymptotic behavior has been confirmed in various many-body models [24, 32, 48, 49].

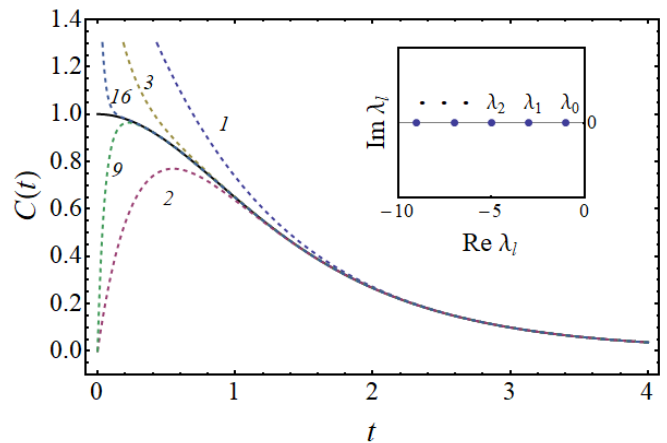


FIG. 1. Pseudomode expansion for the toy model. Solid line – exact autocorrelation function (9). Dashed lines – the pseudomode expansion (12) truncated at various orders l_{\max} (indicated by numbers). Inset – the pseudomode spectrum of the model.

Pseudomode expansion. A well-known strategy to improve an approximate solution of a dynamical equation is to add an artificial dissipation and then to consider the limit of the vanishing dissipation strength [2, 8, 9, 36–39]. We implement this general idea by introducing diagonal terms

$$a_n = \begin{cases} 0, & n \leq n_{\max} \\ i\gamma(n - n_{\max}), & n \geq n_{\max} + 1 \end{cases} \quad (4)$$

in the evolution superoperator (2), where $\gamma > 0$ is the dissipation strength.

There are good reasons to choose this particular form of artificial dissipation. First of all, any self-adjoint superoperator of Markovian dissipative evolution can be brought to the tridiagonal form (2) [42, 44]. Further, first $(n_{\max} + 1)$ derivatives of $C(t)$ at $t = 0$ remain unaltered by the artificial dissipation (4), thanks to zero diagonal terms. Therefore the artificial dissipation does not alter the initial behavior of the correlation function which is known to be reproduced extremely accurately by the recursion method [32].

Finally and most importantly, the linear growth of a_n at large n conforms with the dissipative version of the UOGH that is believed to be valid for generic Markovian dissipative systems [42–44]. A remarkable feature of such systems is the localization of eigenvectors of \mathcal{L} in the Krylov space [43] (see also [44], [18]).¹

¹ A different mechanism for Krylov localization was proposed in ref. [50] (see also [27, 28]) – an Anderson-type localization in the absence of dissipation due to the disorder in the subleading terms of the Lanczos coefficients. Our experience with specific systems [32] suggests that while such a disorder is indeed present, it may not be strong enough to cause localization for generic systems and observables.

Let us discuss the above localization in more detail. Generically, \mathcal{L} is diagonalizable,

$$i\mathcal{L}\mathcal{U} = \mathcal{U}\Lambda, \quad (5)$$

where \mathcal{U} is an invertible matrix with column vectors being eigenvectors of \mathcal{L} , and $\Lambda = \text{diag}(\lambda_0, \lambda_1, \lambda_2, \dots)$ is the diagonal matrix of the corresponding eigenvalues. Since $\mathcal{L} = \mathcal{L}^\top$, one can choose \mathcal{U} such that $\mathcal{U}^{-1} = \mathcal{U}^\top$, which is equivalent to normalizing \mathcal{U} according to $\mathcal{U}^\top\mathcal{U} = \mathbf{1}$ [18]. We employ such normalization in what follows.

The eigenvalues are either real or come in complex-conjugate pairs. In any case $\text{Re } \lambda_l \leq 0$. We order the eigenvalues by the ascending absolute values of their real parts (complex-conjugate pairs $(\lambda_l, \lambda_{l+1} = \lambda_l^*)$ are additionally ordered according to $\text{Im } \lambda_l < 0$), see Figs. 1,2.

The localization implies that, for any finite γ ,

- the spectrum $\{\lambda_0, \lambda_1, \lambda_2, \dots\}$ of \mathcal{L} is discrete and
- the eigenvectors of \mathcal{L} are localized, $|\mathcal{U}_l^n| < e^{-\kappa_l|n-l|}$, where $\kappa_l > 0$ is the inverse localization length.

Our central set of assumptions that underlie the pseudomode expansion concerns the behavior of λ_l and \mathcal{U}_l^0 in the limit $\gamma \rightarrow +0$ of the vanishing dissipation strength. Namely, we assume that

- $\lim_{\gamma \rightarrow +0} \mathcal{U}_l^0$ exists for all l , is bounded in absolute value by a constant independent of l and is nonzero at least for some l ;
- $\lim_{\gamma \rightarrow +0} \lambda_l$ exists and has a strictly negative real part for all l^2 (this statement has been recently rigorously proven for a certain random circuit [51]);
- the spectrum remains discrete, i.e.

$$\lim_{\gamma \rightarrow +0} (\lambda_l - \lambda_{l'}) \neq 0 \quad \text{for } l \neq l'. \quad (6)$$

The above assumptions will be verified in a toy model of \mathcal{L} and in two microscopic spin models, see Figs. 1,2. The two assumptions concerning λ_l essentially coincide with those underlying quantum many-body Ruelle-Pollicott resonances [2, 8, 9]. Note that while localization of $\lim_{\gamma \rightarrow +0} \mathcal{U}_l^0$ is not strictly necessary for the pseudomode expansion, as illustrated below in a toy model, such localization is expected generically and is indeed found in microscopic models.

² In general, the latter requirement can be relaxed for the leading pseudomode λ_0 , which can converge to zero. This would imply that $C(t)$ converges to a nonzero value in the limit $t \rightarrow \infty$. We do not address this case in the present paper, leaving it for further studies.

After a standard algebra, one obtains $O_t = \mathcal{U} e^{\Lambda t} \mathcal{U}^\top O$ and hence

$$C(t) = \sum_{l=0}^{\infty} (\mathcal{U}_l^0)^2 e^{\lambda_l t}. \quad (7)$$

In this formula, \mathcal{U}_l^0 and λ_l should be understood as limiting values at $\gamma \rightarrow +0$. We refer to eq.(7) as the pseudomode expansion. Crucially, the pseudomode expansion is a discrete sum, thanks to the assumption (6).

To the best of our knowledge, the pseudomode expansion (7) first appeared in the 1965 paper by Hazime Mori [1], exactly in the context of the recursion method. However, his approach to computing pseudomode eigenvalues and amplitudes (known as “ n -pole approximation” [22]) was based on assumptions that were, in fact, never satisfied in generic many-body systems. Later the pseudomode expansion (7) recurrently reappeared in various other contexts [7, 9, 12, 14, 16, 18].

For a nonintegrable many-body system, one is able to accurately compute only a finite number of terms in eq. (7). Fortunately, the pseudomode expansion typically converges very fast, as illustrated by examples below. As a result, the *truncated* pseudomode expansion containing only a small number $l = l_{\text{max}}$ of the terms in the sum (7) can deliver a very good approximation to the actual correlation function. Note that the asymptotic behavior of the autocorrelation function at $t \rightarrow \infty$ is, in general, determined by the leading eigenvalue λ_0 in case of $\text{Im } \lambda_0 = 0$, or by the leading pair of complex conjugate eigenvalues $\lambda_0 = \lambda_1^*$ otherwise.

Toy model. Here we consider a toy evolution superoperator [24, 44, 52, 53] with

$$b_n = \sqrt{1 - \gamma^2} n, \quad a_n = i\gamma(2n + 1). \quad (8)$$

While it is not obtained from any known microscopic many-body model, it is believed to grasp some of the major general features of actual evolution operators, since the sequences of b_n and a_n follow the UOGH [24, 42–44].

Note that coefficients a_n in eq. (8) are not exactly of the form (4). Most importantly, they do not vanish for any $n > 0$. The consequence of this fact will be discussed below.

The set (3) of Heisenberg equations for this toy \mathcal{L} can be explicitly solved with the result [24, 44, 52, 53]

$$C(t) = \frac{1}{\cosh(t) (1 + \gamma \tanh(t))} \xrightarrow{\gamma \rightarrow 0} \frac{1}{\cosh(t)}. \quad (9)$$

Our goal is to reproduce this autocorrelation function by means of the pseudomode expansion (7).

This task can be easily completed since the spectrum and the eigenvectors of \mathcal{L} can be explicitly computed for

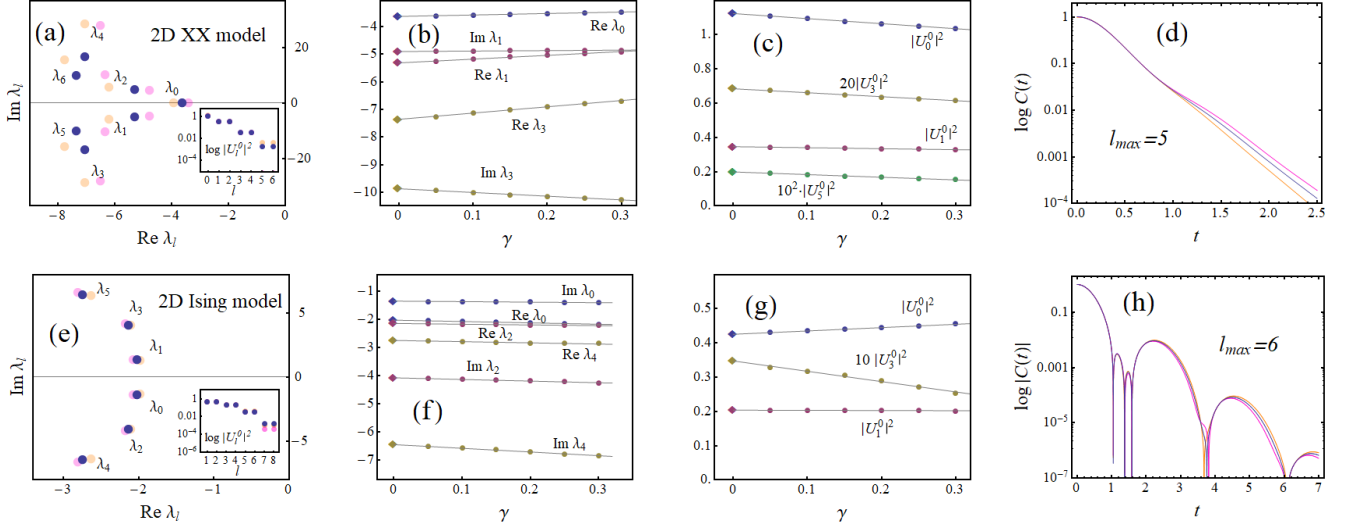


FIG. 2. Pseudomode spectra and expansions for two quantum spin-1/2 models on a square lattice: upper row – XX model (13), lower row – Ising model (14). (a),(e): The rightmost part of the pseudomode spectrum; the inset shows the pseudomode amplitudes. Points of different colors correspond to different ways to extrapolate the Lanczos coefficients; their spread reflects the uncertainty due to the extrapolation error (see Supplemental Material [52] for details). (b),(f) and (c),(g): The convergence of pseudomode eigenvalues and amplitudes, respectively, in the limit of vanishing dissipation strength γ . Points indicate the values obtained for finite γ in the numerical thermodynamic limit (see Supplemental Material [52] for details). Diamonds correspond to the limit of $\gamma \rightarrow 0$ obtained by extrapolation (lines). (d),(h): The autocorrelation function $C(t)$ computed by means of the truncated pseudomode expansion with l_{\max} pseudomodes. Different lines indicate the effect of the error in Lanczos coefficient extrapolation, with the color code consistent with (a),(e). Note that in the Ising model $C(t)$ has alternating sign, for this reason it is the absolute value of $C(t)$ which is plotted in (h).

$\gamma \in (0, 1)$ [24, 44, 52, 53]:

$$\lambda_l = -(2l + 1), \quad (10)$$

$$U_l^0 = \sqrt{\frac{2}{1+\gamma}} (-i)^l \left(\frac{1-\gamma}{1+\gamma} \right)^{l/2} \xrightarrow{\gamma \rightarrow +0} \sqrt{2} (-i)^l. \quad (11)$$

All eigenvalues are real negative and do not depend on γ , and U_l^0 are well-defined in the limit of vanishing dissipation strength. Hence our assumptions are satisfied and the pseudomode expansion (7) reads

$$C(t) = \frac{1}{\cosh(t)} = 2 \sum_{l=0}^{\infty} (-1)^l e^{-(2l+1)t}. \quad (12)$$

The eigenvectors (11) exhibit localization for any finite γ (see [52] for details) but not in the limit of vanishing γ . Still, the sum in eq. (12) converges for any fixed $t > 0$, thanks to the linear growth of λ_l with l . This is illustrated in Fig. 1, where the truncated pseudomode expansion is compared to the actual value of $C(t)$ for various truncation orders l_{\max} . One can see that the convergence is spectacular at intermediate and large times. In particular, the leading pseudomode correctly reproduces the asymptotic behavior $C(t) \sim 2e^{-t}$ at large times. However, the convergence worsens at small times and is absent at $t = 0$. This is not surprising, since the small-time behavior is expected to be reproduced pro-

vided coefficients a_n vanish for first few n , which is not the case in this toy model.

Spin models. Here we consider two nearest-neighbour spin-1/2 models on the square lattice, the XX model and the transverse field Ising model, with respective Hamiltonians given by

$$H_{XX} = \sum_{\langle \mathbf{ij} \rangle} (\sigma_i^x \sigma_j^x + \sigma_i^y \sigma_j^y). \quad (13)$$

$$H_{\text{Ising}} = \sum_{\langle \mathbf{ij} \rangle} \sigma_i^x \sigma_j^x + \sum_{\mathbf{j}} \sigma_j^z, \quad (14)$$

Here \mathbf{i} and \mathbf{j} label lattice sites and the sum over $\langle \mathbf{ij} \rangle$ runs over bonds connecting neighbouring sites.

For both models we choose the observable

$$A = \sum_{\substack{\langle \mathbf{ij} \rangle \\ \mathbf{i} < \mathbf{j}}} (\sigma_i^x \sigma_j^y - \sigma_j^x \sigma_i^y), \quad (15)$$

where the sum runs over horizontal bonds, the site \mathbf{i} being always to the left of the site \mathbf{j} . Up to multiplicative constants, this observable has the meaning of the energy current for the Ising model and the spin current for the XX model.

To obtain the pseudomode expansion of the autocorrelation function, we proceed in several steps. First, we explicitly compute $n_{\max} = 11$ Lanczos coefficients b_n for

the XX model [52] and $n_{\max} = 21$ – for the Ising model [32, 52].

Next, using n_{\max} first Lanczos coefficients, we extrapolate the subsequent coefficients linearly, in accordance with the UOGH. Details of the extrapolation procedure and an estimate of the extrapolation error can be found in the Supplement [52].

Next we choose some finite $\gamma > 0$ and thus fix the diagonal coefficients a_n according to eq. (4). Then we truncate the infinite matrix \mathcal{L} at some size k (note that this truncation is unrelated to the truncation of the pseudomode expansion (7)) and compute its eigenvalues $\lambda_l(\gamma, k)$ and eigenvectors $\mathcal{U}_l^n(\gamma, k)$ by numerical diagonalization. By repeating the latter step for larger and larger k , we numerically take the limit of $k \rightarrow \infty$ and obtain $\lambda_l(\gamma) = \lim_{k \rightarrow \infty} \lambda_l(\gamma, k)$ and $\mathcal{U}_l^0(\gamma) = \lim_{k \rightarrow \infty} \mathcal{U}_l^n(\gamma, k)$. The convergence is fast thanks to the localization: essentially, the limit is saturated for $k \gtrsim \kappa_l^{-1} + l$ [52].

Finally, by repeating the above procedure for a range of $\gamma > 0$, we numerically compute eigenvalues $\lambda_l = \lim_{\gamma \rightarrow +0} \lambda_l(\gamma)$ and amplitudes $\mathcal{U}_l^0 = \lim_{\gamma \rightarrow +0} \mathcal{U}_l^n(\gamma)$ for l_{\max} first pseudomodes, as illustrated in 2 (b),(c),(f),(g). Plugging them in eq. (7) and truncating the sum at $l = l_{\max}$, we get the truncated pseudomode expansion of the autocorrelation function.

Remarkably, in contrast to the toy model, here the localization of eigenvectors survives the limit of vanishing coupling, and pseudomode amplitudes $(\mathcal{U}_l^0)^2$ decay exponentially with l , as can be seen from insets in Fig. 2 (a),(e). This dramatically increases the rate of convergence of the pseudomode expansion. In fact, it turns out that a correlation function can be accurately approximated by a sum of only a few first pseudomodes, as illustrated in Fig. 2 (d),(h).

The latter fact is quite fortunate, since the uncertainty in extrapolating the sequence of Lanczos coefficients limits the accuracy of the computed pseudomodes eigenvalues λ_l and amplitudes \mathcal{U}_l^0 , and the corresponding error grows with l , as illustrated in Fig 2 (a),(e). As a result, in practice only a finite number of first pseudomodes can be reliably recovered for a finite n_{\max} . Naturally, this number grows when n_{\max} is increased.

Summary. To summarize, our studies confirm a long-standing surmise [1–4, 8, 9] that a time-dependent correlation function of a generic many-body system can be accurately approximated by a linear combination of a few pseudomodes $e^{\lambda_l t}$ with complex eigenvalues λ_l . We have presented an algorithmic way to compute pseudomode eigenvalues and amplitudes starting from the Lanczos coefficients obtained within the recursion method. We have applied the method to two quantum spin models on a square lattice. In these examples, the knowledge of a dozen or two of first Lanczos coefficients is enough to find a few first pseudomodes and compute the autocorrelation function with a good accuracy.

Note added. After the first version of the present manuscript had been posted to arXiv and submitted to the journal, five papers [54–58] pursuing a closely related agenda appeared. Various systems were addressed there, including the Sachdev-Ye-Kitaev model [54], one-dimensional kicked Ising model [55] and random unitary circuits [56–58].

Acknowledgments. We thank Boris Fine, Nikolay Il'in, Alexander Jacoby and Matthew Dodelson for valuable discussions. This work was supported by the Russian Science Foundation under grant № 24-22-00331, <https://rscf.ru/en/project/24-22-00331/>

-
- [1] Hazime Mori, “A continued-fraction representation of the time-correlation functions,” *Progress of Theoretical Physics* **34**, 399–416 (1965).
 - [2] Tomaz Prosen, “Ruelle resonances in quantum many-body dynamics,” *Journal of Physics A: Mathematical and General* **35**, L737 (2002).
 - [3] Boris V. Fine, “Long-time relaxation on spin lattice as a manifestation of chaotic dynamics,” *International Journal of Modern Physics B* **18**, 1119–1159 (2004).
 - [4] Boris V. Fine, “Long-time behavior of spin echo,” *Phys. Rev. Lett.* **94**, 247601 (2005).
 - [5] S. W. Morgan, B. V. Fine, and B. Saam, “Universal long-time behavior of nuclear spin decays in a solid,” *Phys. Rev. Lett.* **101**, 067601 (2008).
 - [6] E. G. Sorte, B. V. Fine, and B. Saam, “Long-time behavior of nuclear spin decays in various lattices,” *Phys. Rev. B* **83**, 064302 (2011).
 - [7] Benno Meier, Jonas Kohlrantz, and Jürgen Haase, “Eigenmodes in the long-time behavior of a coupled spin system measured with nuclear magnetic resonance,” *Phys. Rev. Lett.* **108**, 177602 (2012).
 - [8] Tomaz Prosen, “Chaos and complexity of quantum motion,” *Journal of Physics A: Mathematical and Theoretical* **40**, 7881 (2007).
 - [9] Takashi Mori, “Liouvillian-gap analysis of open quantum many-body systems in the weak dissipation limit,” *Phys. Rev. B* **109**, 064311 (2024).
 - [10] B. M. Garraway and P. L. Knight, “Cavity modified quantum beats,” *Physical Review A* **54**, 3592 (1996).
 - [11] B. M. Garraway, “Nonperturbative decay of an atomic system in a cavity,” *Physical Review A* **55**, 2290 (1997).
 - [12] B. J. Dalton, Stephen M. Barnett, and Barry M. Garraway, “Theory of pseudomodes in quantum optical processes,” *Physical Review A* **64**, 053813 (2001).
 - [13] Dario Tamascelli, Andrea Smirne, Susana F. Huelga, and Martin B. Plenio, “Nonperturbative treatment of non-markovian dynamics of open quantum systems,” *Physical Review Letters* **120**, 030402 (2018).
 - [14] Aleksandr E. Teretenkov, “Pseudomode approach and vibronic non-markovian phenomena in light-harvesting complexes,” *Proceedings of the Steklov Institute of Mathematics* **306**, 242–256 (2019).
 - [15] Dario Tamascelli, Andrea Smirne, James Lim, Susana F. Huelga, and Martin B. Plenio, “Efficient simulation of finite-temperature open quantum systems,” *Physical Re-*

- view *Letters* **123**, 090402 (2019).
- [16] Graeme Pleasance, Barry M. Garraway, and Francesco Petruccione, “Generalized theory of pseudomodes for exact descriptions of non-markovian quantum processes,” *Physical Review Research* **2**, 043058 (2020).
- [17] Kiyoshi Kanazawa and Didier Sornette, “Standard form of master equations for general non-markovian jump processes: The laplace-space embedding framework and asymptotic solution,” *Physical Review Research* **6**, 023270 (2024).
- [18] Alexander Teretenkov and Oleg Lychkovskiy, “Exact dynamics of quantum dissipative XX models: Wannier-Stark localization in the fragmented operator space,” *Physical Review B* **109**, L140302 (2024).
- [19] David Ruelle, “Resonances of chaotic dynamical systems,” *Phys. Rev. Lett.* **56**, 405–407 (1986).
- [20] Mark Pollicott, “On the rate of mixing of axiom a flows,” *Inventiones mathematicae* **81**, 413–426 (1985).
- [21] Marc Dupuis, “Moment and continued fraction expansions of time autocorrelation functions,” *Progress of Theoretical Physics* **37**, 502–537 (1967).
- [22] VS Viswanath and Gerhard Müller, *The Recursion Method: Application to Many-Body Dynamics*, Vol. 23 (Springer Science & Business Media, 2008).
- [23] Pratik Nandy, Apollonas S Matsoukas-Roubeas, Pablo Martínez-Azcona, Anatoly Dymarsky, and Adolfo del Campo, “Quantum dynamics in krylov space: Methods and applications,” arXiv preprint arXiv:2405.09628 (2024).
- [24] Daniel E. Parker, Xiangyu Cao, Alexander Avdoshkin, Thomas Scaffidi, and Ehud Altman, “A universal operator growth hypothesis,” *Phys. Rev. X* **9**, 041017 (2019).
- [25] Iliia Khait, Snir Gazit, Norman Y. Yao, and Assa Auerbach, “Spin transport of weakly disordered heisenberg chain at infinite temperature,” *Phys. Rev. B* **93**, 224205 (2016).
- [26] Wesley Luiz de Souza, Érica de Mello Silva, and Paulo H. L. Martins, “Dynamics of the spin-1/2 ising two-leg ladder with four-spin plaquette interaction and transverse field,” *Phys. Rev. E* **101**, 042104 (2020).
- [27] Daniel J. Yates, Alexander G. Abanov, and Aditi Mitra, “Lifetime of almost strong edge-mode operators in one-dimensional, interacting, symmetry protected topological phases,” *Phys. Rev. Lett.* **124**, 206803 (2020).
- [28] Daniel J. Yates, Alexander G. Abanov, and Aditi Mitra, “Dynamics of almost strong edge modes in spin chains away from integrability,” *Phys. Rev. B* **102**, 195419 (2020).
- [29] Xiao-Juan Yuan, Jing-Fen Zhao, Hui Wang, Hong-Xia Bu, Hui-Min Yuan, Bang-Yu Zhao, and Xiang-Mu Kong, “Spin dynamics of an ising chain with bond impurity in a tilt magnetic field,” *Physica A: Statistical Mechanics and its Applications* **583**, 126279 (2021).
- [30] Jiaozi Wang, Mats H. Lamann, Robin Steinigeweg, and Jochen Gemmer, “Diffusion constants from the recursion method,” *Phys. Rev. B* **110**, 104413 (2024).
- [31] Christian Bartsch, Anatoly Dymarsky, Mats H. Lamann, Jiaozi Wang, Robin Steinigeweg, and Jochen Gemmer, “Estimation of equilibration time scales from nested fraction approximations,” *Phys. Rev. E* **110**, 024126 (2024).
- [32] Filipp Uskov and Oleg Lychkovskiy, “Quantum dynamics in one and two dimensions via the recursion method,” *Phys. Rev. B* **109**, L140301 (2024).
- [33] Sauri Bhattacharyya, Ayush De, Snir Gazit, and Assa Auerbach, “Metallic transport of hard-core bosons,” *Phys. Rev. B* **109**, 035117 (2024).
- [34] Richard D Mattuck, *A guide to Feynman diagrams in the many-body problem* (Courier Corporation, 1992).
- [35] Dmitrii N Zubarev, Vladimir G Morozov, and Gerd Röpke, *Statistical Mechanics of Nonequilibrium Processes, Volume 1 (See 3527400834): Basic Concepts, Kinetic Theory*, Vol. 1 (Wiley-VCH, 1996).
- [36] Tibor Rakovszky, C. W. von Keyserlingk, and Frank Pollmann, “Dissipation-assisted operator evolution method for capturing hydrodynamic transport,” *Phys. Rev. B* **105**, 075131 (2022).
- [37] Christopher David White, “Effective dissipation rate in a liouvillian-graph picture of high-temperature quantum hydrodynamics,” *Phys. Rev. B* **107**, 094311 (2023).
- [38] Stuart Yi-Thomas, Brayden Ware, Jay D. Sau, and Christopher David White, “Comparing numerical methods for hydrodynamics in a one-dimensional lattice spin model,” *Phys. Rev. B* **110**, 134308 (2024).
- [39] En-Jui Kuo, Brayden Ware, Peter Lunts, Mohammad Hafezi, and Christopher David White, “Energy diffusion in weakly interacting chains with fermionic dissipation-assisted operator evolution,” arXiv preprint arXiv:2311.17148 (2023).
- [40] Tim Byrnes Igor Ermakov, Oleg Lychkovskiy, “Unified framework for efficiently computable quantum circuits,” arXiv preprint arXiv:2401.08187 (2024).
- [41] NS Srivatsa, Oliver Lunt, Tibor Rakovszky, and Curt von Keyserlingk, “Probing hydrodynamic crossovers with dissipation-assisted operator evolution,” arXiv:2408.08249 (2024).
- [42] Aranya Bhattacharya, Pratik Nandy, Pingal Pratyush Nath, and Himanshu Sahu, “Operator growth and krylov construction in dissipative open quantum systems,” *Journal of High Energy Physics* **2022**, 1–31 (2022).
- [43] Chang Liu, Haifeng Tang, and Hui Zhai, “Krylov complexity in open quantum systems,” *Phys. Rev. Res.* **5**, 033085 (2023).
- [44] Budhaditya Bhattacharjee, Xiangyu Cao, Pratik Nandy, and Tanay Pathak, “Operator growth in open quantum systems: lessons from the dissipative SYK,” *Journal of High Energy Physics* **2023**, 1–29 (2023).
- [45] Jian-Min Liu and Gerhard Müller, “Infinite-temperature dynamics of the equivalent-neighbor xyz model,” *Phys. Rev. A* **42**, 5854–5864 (1990).
- [46] VE Zobov and AA Lundin, “Second moment of multiple-quantum nmr and a time-dependent growth of the number of multispin correlations in solids,” *Journal of Experimental and Theoretical Physics* **103**, 904–916 (2006).
- [47] Tarek A. Elsayed, Benjamin Hess, and Boris V. Fine, “Signatures of chaos in time series generated by many-spin systems at high temperatures,” *Phys. Rev. E* **90**, 022910 (2014).
- [48] Jae Dong Noh, “Operator growth in the transverse-field ising spin chain with integrability-breaking longitudinal field,” *Phys. Rev. E* **104**, 034112 (2021).
- [49] Ayush De, Umberto Borla, Xiangyu Cao, and Snir Gazit, “Stochastic sampling of operator growth dynamics,” *Phys. Rev. B* **110**, 155135 (2024).
- [50] E Rabinovici, A Sánchez-Garrido, R Shir, and J Sonner, “Krylov localization and suppression of complexity,” *Journal of High Energy Physics* **2022**, 1–42 (2022).
- [51] Takato Yoshimura and Lucas Sá, “Robustness of quan-

- tum chaos and anomalous relaxation in open quantum circuits,” *Nature Communications* **15**, 9808 (2024).
- [52] See the Supplementary Material for the details on the the toy evolution operator and on application of the developed technique to microscopic Hamiltonians. The Supplementary Material contains ref. [59].
- [53] Vijay Balasubramanian, Pawel Caputa, Javier M. Magan, and Qingyue Wu, “Quantum chaos and the complexity of spread of states,” *Phys. Rev. D* **106**, 046007 (2022).
- [54] Matthew Dodelson, “Ringdown in the syk model,” arXiv preprint arXiv:2408.05790 (2024).
- [55] Marko Žnidarič, “Momentum-dependent quantum ruelle-pollicott resonances in translationally invariant many-body systems,” *Phys. Rev. E* **110**, 054204 (2024).
- [56] J Alexander Jacoby, David A Huse, and Sarang Gopalakrishnan, “Spectral gaps of local quantum channels in the weak-dissipation limit,” arXiv preprint arXiv:2409.17238 (2024).
- [57] Carolyn Zhang, Laimei Nie, and Curt von Keyserlingk, “Thermalization rates and quantum ruelle-pollicott resonances: insights from operator hydrodynamics,” arXiv preprint arXiv:2409.17251 (2024).
- [58] Takato Yoshimura and Lucas Sá, “Theory of irreversibility in quantum many-body systems,” arXiv preprint arXiv:2501.06183 (2025).
- [59] Luigi Accardi, Uwe Franz, and Michael Skeide, “Renormalized squares of white noise and other non-gaussian noises as lévy processes on real lie algebras,” *Communications in Mathematical Physics* **228**, 123–150 (2002).

Supplementary material
to the Letter
“Pseudomode expansion of many-body correlation functions”
by Alexander Teretenkov, Filipp Uskov and Oleg Lychkovskiy.

S1. Toy model

The toy evolution operator (2),(8) can be represented as

$$\mathcal{L} = i\gamma M + \sqrt{1 - \gamma^2}(B + B^\dagger), \quad (\text{S1})$$

where

$$M = \begin{pmatrix} 1 & 0 & 0 & 0 & \dots \\ 0 & 3 & 0 & 0 & \dots \\ 0 & 0 & 5 & 0 & \dots \\ 0 & 0 & 0 & 7 & \dots \\ \vdots & \vdots & \vdots & \vdots & \ddots \end{pmatrix}, \quad B = \begin{pmatrix} 0 & 1 & 0 & 0 & \dots \\ 0 & 0 & 2 & 0 & \dots \\ 0 & 0 & 0 & 3 & \dots \\ 0 & 0 & 0 & 0 & \dots \\ \vdots & \vdots & \vdots & \vdots & \ddots \end{pmatrix}. \quad (\text{S2})$$

Crucially, operators M and B satisfy

$$[B, B^\dagger] = M, \quad [B, M] = 2B, \quad [B^\dagger, M] = -2B^\dagger, \quad (\text{S3})$$

cf. ref. [59]. These commutation relations can be easily obtained from the action of the above operators on basis vectors $|n\rangle$, $n = 0, 1, 2, \dots$:

$$B|n\rangle = n|n-1\rangle, \quad B^\dagger|n\rangle = (n+1)|n+1\rangle, \quad M|n\rangle = (2n+1)|n\rangle. \quad (\text{S4})$$

Using commutation relations (S3), one brings \mathcal{L} to the diagonal form as follows:

$$\mathcal{L} = e^{i\tau(\gamma)(B^\dagger - B)}(iM)e^{-i\tau(\gamma)(B^\dagger - B)}, \quad (\text{S5})$$

where

$$\tau(\gamma) = \arccos\left(-\sqrt{\frac{1+\gamma}{2}}\right), \quad \gamma \in (0, 1). \quad (\text{S6})$$

Thus \mathcal{U} and Λ from eq. (5) read

$$\mathcal{U} = e^{i\tau(\gamma)(B^\dagger - B)}, \quad \Lambda = -M. \quad (\text{S7})$$

Eigenvalues (10) follow immediately. Eigenvectors (11) and autocorrelation function (9) are obtained after some straightforward algebra.

S2. Pseudomodes in the XX and Ising models on the square lattice

S2.1. Computing n_{\max} first Lanczos coefficients

We use a computer program reported in ref. [32] to compute n_{\max} first moments and Lanczos coefficient. We are able to achieve $n_{\max} = 11$ for the XX model and $n_{\max} = 21$ for the Ising model. The results are shown in Table S1 and Table S2, respectively. The Lanczos coefficients are also shown in Fig. S1(a),(d).

n	μ_{2n}	b_n
1	16	4.0
2	1024	6.9282
3	136192	9.5917
4	30277632	12.2131
5	9983098880	14.5925
6	4498943967232	16.6669
7	2599858319392768	18.1310
8	1834298158063026176	19.9233
9	1527776305296896425984	22.1031
10	1472244134830457072123904	24.0962
11	1624011303835553036301762560	25.8961

TABLE S1. Moments and Lanczos coefficients for the XX model on the square lattice, eq. (13), and observable (15).

n	μ_{2n}	b_n
1	8	2.8284
2	192	4.0
3	8192	5.2915
4	546816	6.7612
5	53321728	8.0861
6	7175143424	9.3673
7	1268516651008	10.6283
8	282984740552704	11.7194
9	77099370874404864	12.8275
10	24994506356392198144	13.9370
11	9447181150949853888512	14.9831
12	4097682751836764564881408	15.8407
13	2013581261449707414815244288	16.6125
14	1108435050944563799272751890432	17.3425
15	676413174916563342565009178755072	18.2729
16	453089374036703756783428077313064960	19.1098
17	330151040493164361120913228230360563712	19.9837
18	259674454740125766898519426917750737469440	20.7966
19	219085451111188700544806075134247988359069696	21.6735
20	197334932443983424783725995684533384746838786048	22.5520
21	189115452873144653249584832927971057967336192475136	23.4344

TABLE S2. Moments and Lanczos coefficients for the Ising model on the square lattice, eq. (14), and observable (15).

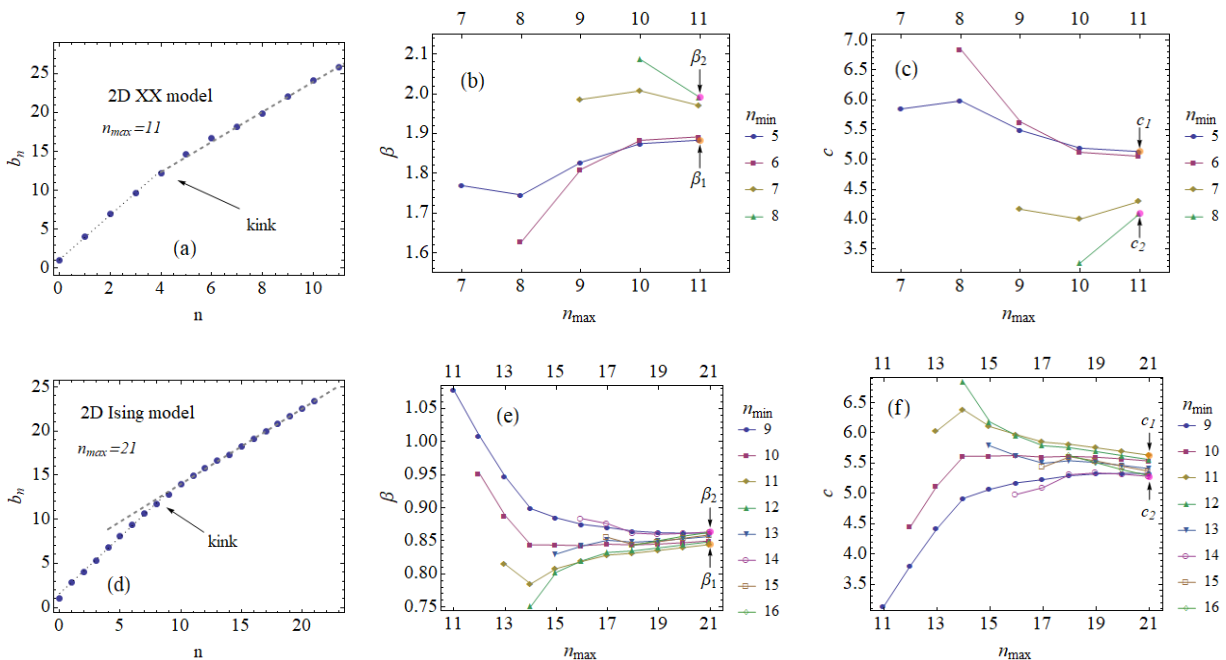


FIG. S1. Lanczos coefficients and linear fits to these coefficients for the XX (upper row) and the Ising (lower row) models on the square lattice. (a),(d): n_{\max} Lanczos coefficients b_n are shown by blue points, linear fit to these coefficients is shown with a gray dashed line. One can see a kink separating two regions with different slopes. Only points to the right of the kink are used for the fit. (b),(c),(e),(f): Dependence of fitting parameters on the maximal number n_{\max} of the available moments, for various fitting thresholds n_{\min} . Fitting parameters (β_1, c_1) and (β_2, c_2) used to estimate the uncertainty due to fitting errors are shown, respectively, by large orange and pink points and marked by arrows.

S2.2. Extrapolating further Lanczos coefficients according to the UOGH

We extrapolate Lanczos coefficients b_n for $n > n_{\max}$ according to the UOGH, i.e. linearly:

$$b_n^{\text{extr}} = \beta n + c, \quad n \geq n_{\max} + 1. \quad (\text{S8})$$

Constants β and c are obtained from the least squares fit of b_n for $n_{\min} \leq n \leq n_{\max}$. The choice of n_{\min} is somewhat intricate. Examining the plots of Lanczos coefficients for the two models under consideration, Fig. S1(a),(d), we see that each of them exhibits a kink at some $n = n_{\text{kink}}$. The kink separates two regions of n with apparently different slopes β . The origin of this phenomenon is an interesting open question. We assume that there are no other kinks for $n > n_{\max}$, and thus the Lanczos coefficient for $n_{\text{kink}} \leq n \leq n_{\max}$ can be used for the fit.

With a finite number of explicitly computed Lanczos coefficients available, the values of β and c extracted from the fit are necessarily somewhat off the true asymptotic values. To access the uncertainty of fitted β and c , we perform fits for various $n_{\min} \geq n_{\text{kink}}$ and n_{\max} , with the results shown in Fig. S1(b),(c),(e),(f). For a given n_{\max} , we estimate the uncertainty in determining β and c as the maximal spread of these values for various $n_{\text{kink}} \leq n_{\min} \leq n_{\max} - 2$. This uncertainty tends to decrease with increasing n_{\max} , as can be seen from Fig. S1(b),(c),(e),(f).

To access the effect of extrapolation uncertainty, we compute pseudomodes and autocorrelation functions for three sets of fitting parameters: (β_1, c_1) , (β_2, c_2) and $(\beta_{\text{av}} = (\beta_1 + \beta_2)/2, c_{\text{av}} = (c_1 + c_2)/2)$. The first two fits are extremes obtained by varying n_{\min} , see Fig. S1(b),(c),(e),(f). The third fit is the average of the first two ones. The effect of extrapolation uncertainty on pseudomode eigenvalues is shown in Fig. 2(a),(e) (see also Fig. S2), while the effect on correlation functions – in Fig. 2(d),(h). Whenever not specified explicitly, we use the average fit $(\beta_{\text{av}}, c_{\text{av}})$.

Naturally, the more Lanczos coefficients can be computed explicitly, the less uncertain the fit is and more accurate pseudomode eigenvalues and amplitudes are. We illustrate the accuracy of the pseudomode eigenvalue restoration in Fig. S2.

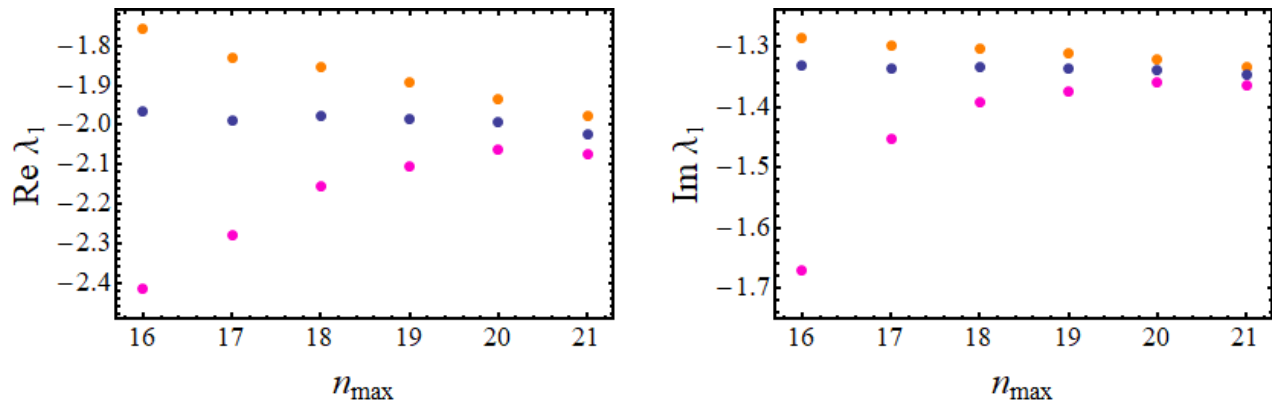


FIG. S2. Extrapolation uncertainty of a pseudomode eigenvalue as a function of the number n_{\max} of explicit Lanczos coefficients available. Shown are real (left) and imaginary (right) parts of the first pseudomode eigenvalue λ_1 for the Ising model on the square lattice. Orange, pink and blue points correspond to fitting parameters (β_1, c_1) , (β_2, c_2) and $(\beta_{\text{av}}, c_{\text{av}})$, respectively. This color code is consistent with that of Fig. S1 and Fig. 2.

S2.3. Taking thermodynamic limit numerically

In Fig. S3 we illustrate our procedure to numerically take the thermodynamic limit. One can see that, for a given γ , the values of $\lambda_l(\gamma, k)$ and $U_l^0(\gamma, k)$ abruptly saturate above some threshold size of the truncated matrix $i\mathcal{L}$. As can be seen from Fig. S3, this threshold size is in fact determined by the support of the corresponding eigenvectors which is finite thanks to the localization.

One may wonder what happens if one takes an “incorrect” order of limits: $\lim_{k \rightarrow \infty} \lim_{\gamma \rightarrow 0} \lambda_l$ instead of $\lim_{\gamma \rightarrow 0} \lim_{k \rightarrow \infty} \lambda_l$. Naturally, in this case eigenvalues would lose their negative real parts and become purely imaginary. Some amazing features of this limit are illustrated in Fig. S4.

S2.4. Comparison between pseudomode expansion and extrapolated recursion method

One can compute the autocorrelation function by extrapolating Lanczos coefficients according to eq. (S8), truncating the system of coupled Heisenberg equations (3) at high $k \sim 1000$ and numerically solving the truncated system [32]. We compare thus computed autocorrelation function with the pseudomode expansion (7) in Fig. S5. One can see that the agreement is good, with the discrepancy between the two approaches not exceeding the uncertainty due to the extrapolation of the Lanczos sequence. We conclude that the two approaches to computing the autocorrelation function have a comparable accuracy.

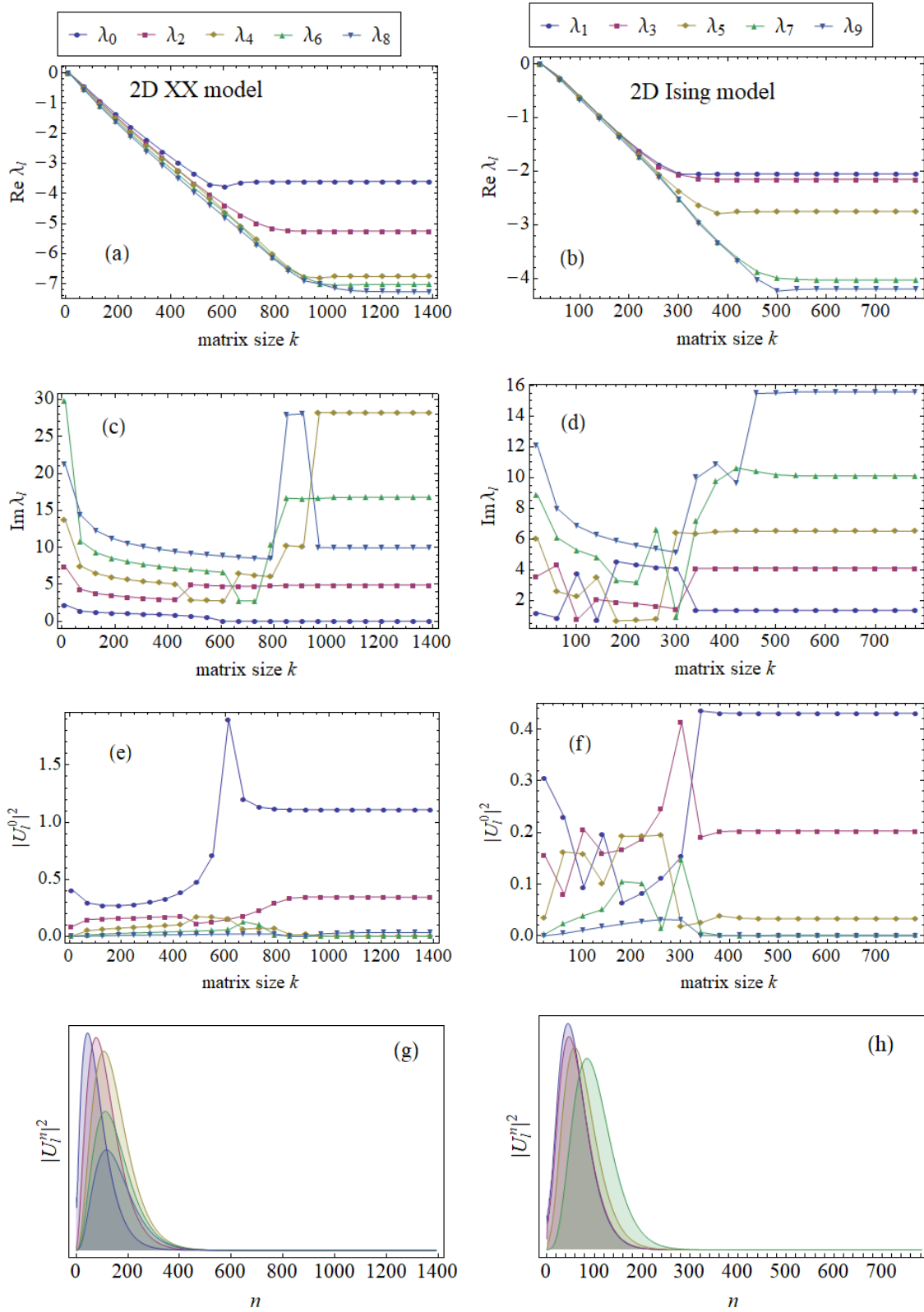


FIG. S3. The numerical thermodynamic limit for pseudomode eigenvalues and amplitudes for a fixed $\gamma = 0.05$. Left (right) column – XX (Ising) model on the square lattice. First two rows show the scaling of, respectively, the real and the imaginary parts of the first few pseudomode eigenvalues $\lambda_l(\gamma, k)$ with the size k of the truncated matrix $i\mathcal{L}$. The third row shows the scaling of the absolute value of the pseudomode amplitudes $|\mathcal{U}_l^0(\gamma, k)|^2$. The fourth row shows the respective full eigenvectors $|\mathcal{U}_l^n(\gamma, 800)|^2$ as functions of n for a fixed truncation size $k = 800$ (the absolute scale is arbitrary for each eigenvector; the color code is consistent with that in other plots). One can see that, thanks to the eigenvector localization, the pseudomode eigenvalues and amplitudes in (a)-(f) are abruptly saturated for k exceeding the support of the respective eigenvectors in (g),(e).

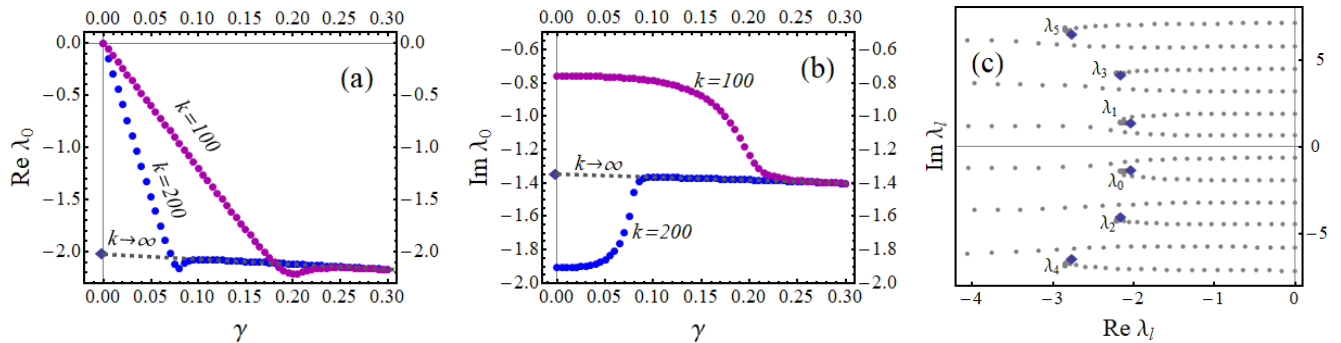


FIG. S4. Dependence of pseudomode eigenvalues on γ for a fixed size k of the truncated matrix $i\mathcal{L}$ in the Ising model. (a) and (b): dependence of the real (a) and imaginary (b) parts of λ_0 on γ for the fixed sizes $k = 200$ (blue points) and $k = 100$ (magenta points). The fit to $k \rightarrow \infty$ is shown by dashed line (see Fig. 2(f),(g)). (c) The flow of eigenvalues with γ for $k = 200$. The value of γ changes from 0 to 0.3, consistent with (a),(b). At zero γ all eigenvalues are purely imaginary. For nonzero γ eigenvalues acquire a negative real part. With the increase of γ , eigenvalues tend to flow to the left. In all three plots blue diamonds mark the “correct” limit $\lim_{\gamma \rightarrow 0} \lim_{k \rightarrow \infty} \lambda_i$ (see Fig. 2(f),(g)). Note that while a half of eigenvalues flow towards the rightmost end of the complex spectrum which we are interested in, the other half quickly flows towards the leftmost part of the spectrum.

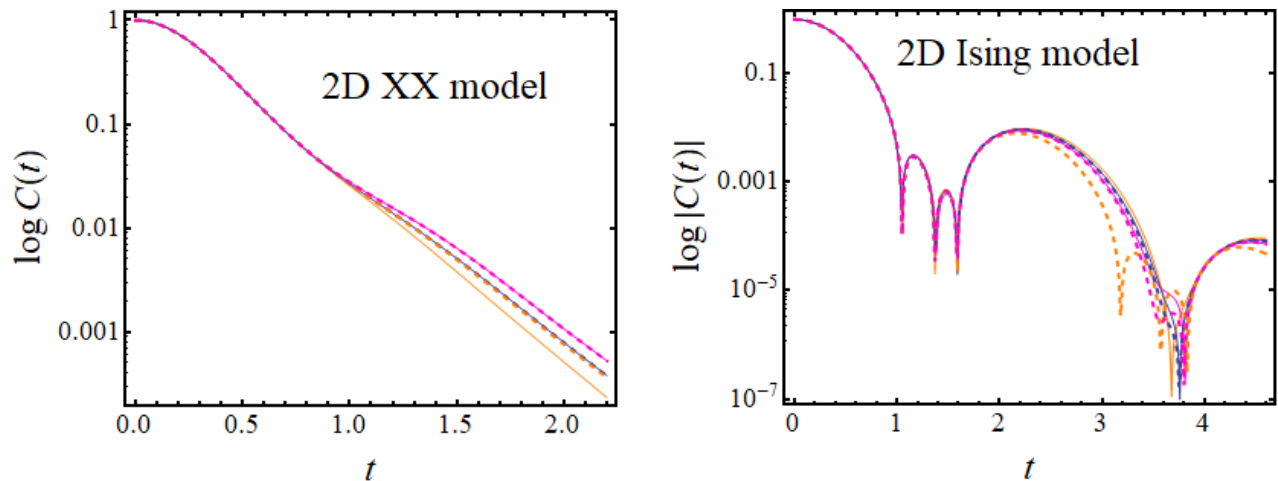


FIG. S5. Correlation function computed by means of the truncated pseudomode expansion (solid) and the extrapolated recursion method [32] with \mathcal{L} truncated at the size $k = 1500$ (dashed). Orange, pink and blue lines correspond to fitting parameters (β_1, c_1) , (β_2, c_2) and (β_{av}, c_{av}) , respectively. This color code is consistent with that of Fig. S1 and Fig. 2.